Spectroscopic Studies of "Exciplex Tuning" for Dicyanoaurate(I) Ions Doped in Potassium Chloride Crystals

Samanthika R. Hettiarachchi,[†] Manal A. Rawashdeh-Omary,[†] Sofian M. Kanan,[†,||] Mohammad A. Omary,[§] Howard H. Patterson,*[,†] and Carl P. Tripp[†,||]

Department of Chemistry, University of Maine, Orono, Maine 04469, Department of Chemistry, P.O. Box 305070, University of North Texas, Denton, Texas 76203, and Laboratory for Surface Science and Technology, University of Maine, Orono, Maine 04469

Received: April 11, 2002; In Final Form: July 15, 2002

Photoluminescence and Raman results for single crystals of KCl doped with $KAu(CN)_2$ with different Au content are presented and compared with results for pure $KAu(CN)_2$ crystals. Photoluminescence spectra of the doped crystals show three major UV−vis bands that can be resolved by varying the excitation wavelength. Spectroscopic and computational evidence suggests the formation of Au−Au bonded excimers and exciplexes in this doped system. The excimer/exciplex luminescence bands can be tuned in a given crystal by site-selective excitation and their relative intensities tuned by varying the dopant concentration. Microsecond lifetimes were observed for the various luminescence bands, suggesting Au-centered phosphorescent emissions. Raman spectral analysis was used successfully to correlate with the luminescence bands observed in pure and doped crystals of $[Au(CN)_2^-]$ and $[Ag(CN)_2^-]$ systems. The Raman *νCN* bands corresponding to various sites of $[Au(CN)_2^-]_n$ and $[Ag(CN)_2^-]_n$ clusters in various crystals correlated well with the luminescence spectra, in terms of both the number of peaks and their relative frequencies. The results have illustrated interesting differences in the clustering of $[Au(CN)_2^-]$ versus $[Ag(CN)_2^-]$ ions in the host lattice. As the dopant level increases, the extent of metal−metal interactions increases due to larger oligomers or shorter metal−metal separation, in either case leading to decreased back-bonding and higher *νCN* frequencies. The *νCN* Raman frequencies in $[Au(CN)_2^-]$/KCl crystals with increasing doping level increased beyond the value for pure $KAu(CN)_2$ crystals, presumably due to a shorter Au−Au distance in the highest doped crystal than the distance in the pure crystal. In contrast, increasing the doping level in $[Ag(CN)_2^-]$/KCl systems resulted in the appearance of *νCN* Raman peaks with correspondingly higher frequencies but the values remained lower than those for pure $KAg(CN)_2$ crystals, as expected.

Introduction

Bonding in compounds of closed shell d^{10} atoms such as gold(I) has attracted the interest of experimental and theoretical chemists because of the remarkable tendency of these compounds to form supramolecular aggregates owing to Au−Au aurophilic bonding.[1,2] A variety of structures showing gold(I) compounds aggregate as dimers, oligomers, and polymers have been reported.[1−8] Che and co-workers have reported a resonance Raman investigation of Au_2[bis(dicyclohexylphosphine)methane]$_2$-$(ClO_4)_2$, which showed Au(I)-Au(I) single bond formation in the excited state.[9a] A further study by the same group has shown that analogous Ag(I) species also give rise to Ag−Ag single bond formation in the excited state.[9b] Our group has recently reported a comparison between Ag−Ag and Au−Au interactions in the ground and excited states of dicyano complexes.[10]

Monovalent gold complexes have been shown to have a variety of applications. For example, $[Au(CN)_2^-]$ ions play an important role in medicinal chemistry.[11] The modern day use of $[Au(CN)_2^-]$ ions for medicinal purposes originated from Robert Koch's discovery, that $[Au(CN)_2^-]$ ions have bacteriostatic properties.[12] It has also been reported that $[Au(CN)_2^-]$ is a common metabolite of injectable gold drugs such as auranofin for the treatment of rheumatoid arthritis.[13] Other potential applications of Au(I) compounds such as in optical sensors,[14] bio-sensors,[15] and photocatalysts[16] provide a strong motivation to study monovalent Au(I) compounds.

Our recent studies of cyano complexes of Au(I) and Ag(I) relate the photoluminescence properties to the formation of metal−metal bonded excimers and exciplexes. Although luminescent exciplexes are well-known molecular entities in the photochemistry and photophysics of organic systems,[17] the field is less common in the inorganic literature and most reported inorganic exciplexes are not luminescent.[18] Metal−metal bonded excimers and exciplexes are the only class of luminescent inorganic exciplexes. Members of this class include homoatomic and heteroatomic exciplexes involving closed shell metal ions, mostly d^8 and d^{10} systems. Examples include those reported by Zink et al. involving $*[Cu^+-Ag^+]$ and $*[Cu^+-Cu^+]$ simple ions in doped β'' alumina;[19,20] also Nagle et al. have reported the existence of Tl^+ bonding to Pt(II) in aqueous solutions of tetrakis(μ-diphosphito)diplatinate(II) and thallium(I),[21a,b] and the formation of Pt(II)−Au(I) bonds in aqueous solutions of $[Au(CN)_2^-]$ and $Pt_2(P_2O_5H_2)^{4-}$.[22] We contributed to this field by introducing the optical phenomenon of "exciplex tuning",

[†] Department of Chemistry, University of Maine.
[§] Department of Chemistry, P.O. Box 305070, University of North Texas.
[||] Laboratory for Surface Science and Technology, University of Maine.

10.1021/jp0209594 CCC: $22.00
Published on Web 09/05/2002

which describes the tuning of the emission in $[Ag(CN)_2^-]$-doped alkali halide crystals to various bands in the ultraviolet and visible regions with each band due to a different oligomeric $*[Ag(CN)_2^-]_n$ excimer or exciplex.[23−26] Tuning the excited state properties is extremely important in a variety of optoelectronic applications in relation to some fundamental scientific issues such as excitonic energy transfer.[27−30] Examples illustrating the significance of exciplex tuning in d^{10} complexes in scientific and practical applications have been reported by some of us regarding tunable energy transfer to lanthanide ions,[31] the photocatalytic action of Ag(I)-doped ZSM-5 zeolites in the decomposition of nitric oxide,[32] and Ag(I)-catalyzed photodecomposition of pesticides.[33,34]

Our group has previously reported luminescence and X-ray measurements versus temperature for pure $KAu(CN)_2$.[35] These results demonstrated the sensitivity of the emission energy to changes in Au−Au separation. Very recently, we have reported the ground and excited-state aurophilic and argentophilic interactions of $[Au(CN)_2^-]_n$ and $[Ag(CN)_2^-]_n$ oligomers in solution.[10,36] We report here the first example of exciplex tuning for $[Au(CN)_2^-]$ ions doped in KCl single crystals. Tuning of the luminescence is studied by site-selective excitation and varying the dopant concentration. By varying the dopant concentration, we have observed from our spectroscopic data an unusual trend: as the dopant concentration increases, the size of the oligomers increases and this is accompanied by a shorter Au−Au bond distance. At the highest dopant concentration, the Au−Au bond distance is shorter than that found in the pure $KAu(CN)_2$ crystal. In contrast, at the highest doping level of the $[Ag(CN)_2^-]$/KCl system, the Ag−Ag bond distance is similar to the same bond length as the corresponding pure crystal. Correlation between the luminescence and Raman bands is made for $M(CN)_2^-$/KCl (M = Au; Ag) doped crystals with varying M content as well as pure crystals of $KM(CN)_2$.

Experimental Section

Single crystals of $KAu(CN)_2$/KCl were grown by slow evaporation of a saturated aqueous solution containing 5 g of KCl and 0.2 g of $KAu(CN)_2$ at ambient temperature. The first batch of $KAu(CN)_2$/KCl crystals was harvested after 4 d of slow evaporation. After harvesting the first batch of crystals (henceforth referred to as "batch 1"), the remaining solution (mother liquor) was allowed to evaporate under ambient conditions. The second batch of $KAu(CN)_2$/KCl crystals (batch 2) was harvested after 6 d. The remaining solution was allowed to evaporate to just before dryness (20 d) at which point, the last batch of crystals (batch 3) was harvested. Pure $KAu(CN)_2$ single crystals were grown from a nearly saturated aqueous solution of $KAu(CN)_2$ and the crystals were harvested after 14 d. Single crystals of $KAg(CN)_2$/KCl were grown using a similar synthetic procedure but using 7.5 g of KCl and 0.5 g of $KAg(CN)_2$. After slow evaporation, the first batch of $KAg(CN)_2$/KCl crystals was harvested after 1 d. The remaining solution was allowed to evaporate longer and, just before dryness, the second batch of $KAg(CN)_2$/KCl crystals was harvested after thirteen days.

The metal content of the different batches of doped crystals was determined using atomic absorption spectroscopy. Atomic absorption measurements were carried out using a Model 857-Smith-Hieftje 11/12 spectrophotometer. To determine the gold content of the different batches of $KAu(CN)_2$/KCl, puro-graphic calibration standards (998 μg/mL gold in 5% HCl) from the Cole−Parmer Company were used as the standard. The crystal growing process was repeated a second time and atomic absorption, luminescence and Raman analyses gave reproducible data. Atomic absorption analyses for different batches of $KAg(CN)_2$/KCl were carried out using puro-graphic calibration standards (995 μg/mL silver in 5% HNO_3).

Raman spectra were obtained using a Raman Imaging Microscope System 1000 equipped with a diode laser operating at $\lambda_{ex} = 785$ nm. All measurements were carried out at room temperature for the same single crystals used in the luminescence measurements.

Steady-state photoluminescence spectra were collected using a Photon Technology International Model QuantaMaster-1046 spectrophotometer equipped with a 75 W Xenon lamp. Wavelengths were selected with two excitation monochromators and a single emission monochromator. All spectra were recorded at 77 K. Excitation spectra were corrected for spectral variation of the lamp using rhodamine B as a quantum counter. Liquid nitrogen was used as the coolant in a Model LT-3-110 Heli-Tran cryogenic liquid transfer system.

Lifetime measurements were recorded using a Nanolaser diode-pumped solid-state laser that pulses at 266 nm with a repetition rate of 8.1 kHz. A 400 MHz LeCroy 9310 digital oscilloscope was used to collect data. The decays were averaged over 1000 sweeps on the oscilloscope. All lifetime measurements were carried out at 77 K.

Computational Details

Ground and first excited-state calculations were carried out using the FORTICON 8 program (QCMP011). Relativistic parameters used for all atoms have been reported previously.[37] Ground and first excited-state calculations were carried out for free monomers, dimers, trimers, and tetramers. Details of the calculations for the free oligomers have been described earlier.[36]

Ground-state calculations were carried out for monomer and eclipsed dimer units of $[Au(CN)_2^-]$ ions doped in a KCl lattice. Upon doping $[Au(CN)_2^-]_n$ ($n = 1,2$) in the KCl lattice, the Au^+ ions replace the K^+ ions and the CN^- ions replace the Cl^- ions. A $[Au(CN)_2^-]$ ion doped in a KCl lattice was modeled by a layer containing a Au^+ ion occupying the site of a K^+ ion with four neighboring Cl^- ions separated by 3.19 Å and four neighboring K^+ ions separated by 4.51 Å.[38] The two CN^- ions were in the perpendicular axis to the plane of the layer described hitherto.

Results and Discussion

Atomic Absorption Results. Pure $KAu(CN)_2$ and three batches isolated from a mixture of $KAu(CN)_2$ and KCl have been studied. Atomic absorption spectroscopy analysis has shown that the values of % Au (by wt) are 0.45, 1.38, and 2.20 for $KAu(CN)_2$/KCl crystals referred to herein as batches 1, 2, and 3, respectively. The variation of Au content among the $KAu(CN)_2$/KCl batches can be explained by the synthetic procedure. The crystals formed in the early stage of slow evaporation of the starting KCl solution contained a low concentration of $[Au(CN)_2^-]$ ions. Therefore, batch 1 has the lowest Au content. After harvesting the first batch of crystals (batch 1), the remaining mother liquor contains a higher concentration of $[Au(CN)_2^-]$ than the starting solution. This leads to KCl crystals grown with a higher gold content in batch 2. Batch 3 has the highest gold content because it is harvested from the most concentrated mother liquor after harvesting batches 1 and 2. Similar arguments also apply for the analogous silver doped system that we are studying in this paper. Atomic absorption analyses of $KAg(CN)_2$/KCl batches 1 and 2 gave 1.21 and 2.23%Ag (wt), respectively.

Steady-State Photoluminescence Spectroscopy. Figure 1 shows the emission spectra of $KAu(CN)_2$/KCl batch 1 at 77 K.

TABLE 1: Correlation of Luminescence and Raman Bands in Various Doped and Pure Crystals of the Dicyanoaurates(I) and Dicyanoargentates(I); Lifetime Measurements were Carried Out at 77 K[a]

	$[Au(CN)_2^-]$/KCl				$[Ag(CN)_2^-]$/KCl	
crystal	emission (excitation) bands, nm	Raman peaks, cm^{-1}	τ (390 nm), μs	τ (425 nm), μs	emission (excitation) bands, nm	Raman peaks, cm^{-1}
batch 1	335 (272), 390 (315), 425 (337)	2169, 2176	0.42 ±0.01	0.92 ±0.01	296 (245), 338 (275), 415 (265)	2118, 2124
batch 2	390 (315)	2176	0.38 ±0.01	–	296 (245), 338 (275), 415 (265)	2118, 2124, 2159
batch 3	335 (272), 390 (315), 425 (337)	2169, 2176, 2189	0.65 ±0.02	1.00 ±0.03		
pure	390 (315)	2176	0.34 ±0.01		415 (265)	2159

[a] Lifetime measurements for doped $[Ag(CN)_2^-]$/KCl crystals were reported in refs 23−26 and they also were in the μs range.

TABLE 2: Summary of the Results of EH Calculations for Ground and First Excited States of Different Oligomers of $[Au(CN)_2^-]_n$ (all with an eclipsed conformation)[a]

species	[Au]	[Au]/KCl	$[Au]_2$/KCl	$[Au]_2$	$^*[Au]_2$	$[Au]_3$ (bent)	$^*[Au]_3$ (bent)	$[Au]_3$ (lin)	$^*[Au]_3$ (lin)	$[Au]_4$ (lin)
d_{Au-Au},A^0			4.51	3.48	3.00	3.48	3.15	3.44	3.08	3.44
B. E., eV			5.1	0.13	0.88	0.266	0.877	0.30	1.2	0.435
H−L gap, eV	4.41	4.09	4.04	3.78	3.41	3.62	3.30	3.43	2.96	3.34
O. P.			−0.0279	0.0226	0.0734	0.0203	0.0679	0.0116	0.0569	0.0098

[a] Notation: $[Au]_{2,3,4} = [Au(CN)_2^-]_{2,3,4}$, $^*[Au]_{2,3}$: excimer/exciplex, lin = linear, B. E. = Au−Au binding energy, H−L gap = HOMO−LUMO gap, O.P = Au−Au overlap population.

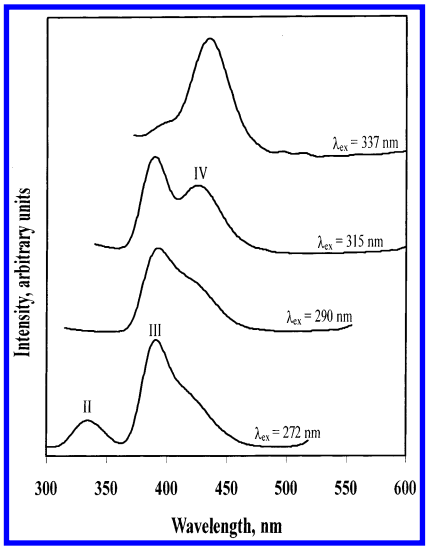

Figure 1. Emission spectra of a single crystal of $KAu(CN)_2$/KCl batch 1 at 77 K with different excitation wavelengths.

Three emission bands at 335, 390, and 425 nm are observed by varying the excitation wavelength in the excitation range 270−350 nm, as illustrated in Figure 1. No other emission bands are observed by varying the excitation wavelength (the two bumps at ∼495 and ∼512 nm are artifacts from the lamp source). The emissions at 335, 390, and 425 nm are henceforth referred to as II, III, and IV, respectively (as shown in Table 3, only $KAu(CN)_2$ solutions shows emission band I).

The corrected excitation spectra of $KAu(CN)_2$/KCl batch 1 at 77 K are shown in Figure 2. Each emission band observed in Figure 1 has a characteristic excitation maximum. Therefore, various emission bands can be resolved by selecting the excitation wavelength. The absorption spectra of infinitesimally dilute aqueous solutions of $KAu(CN)_2$ show a structured profile with $\lambda_{max} \leq 250$ nm.[36,39] All observed excitation bands in the doped $KAu(CN)_2$/KCl (see Figure 2) are at wavelengths longer than 250 nm; this red shift is presumably due to metal−metal interactions. Doped $[Ag(CN)_2^-]$/KCl systems show excitation and emission bands, the low energy of which has been attributed to metal−metal interactions in different aggregations and

TABLE 3: General Qualitative Assignment of the Emission Bands Observed in Solids and Solutions of $Au(CN)_2^-$ Species

band	solids, λ_{max}^{em}, nm	solutions, λ_{max}^{em}, nm	assignment
I		275−285	$^*[Au(CN)_2^-]_2$
II	320−355	320−350	bent$^*[Au(CN)_2^-]_3$
III	370−395	380−390	linear$^*[Au(CN)_2^-]_3$
IV	420−450	420−440	$^*[Au(CN)_2^-]_4$
V		455−490	$^*[Au(CN)_2^-]_n$[a]
VI	600−640		$^*[Au(CN)_2^-]_n$[a]

[a] $^*[Au(CN)_2^-]_n$ represents delocalized exciplexes.

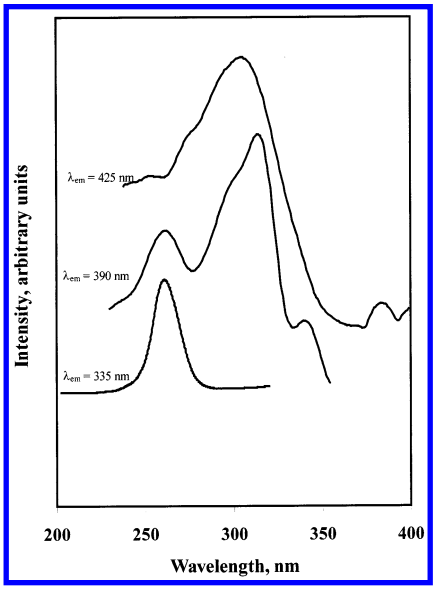

Figure 2. Corrected excitation spectra of a single crystal of $KAu(CN)_2$/KCl batch 1 at wavelengths corresponding to the emission maxima of bands II, III, and IV at 77 K.

orientations of $[Ag(CN)_2^-]$ units.[23,24] Solutions with high concentrations of $[Au(CN)_2^-]$ and $[Ag(CN)_2^-]$ also show similar red shifts in the absorption and emission energies due to oligomerization.[10,36]

Figure 3 shows the emission spectra of batches 1−3 as well as pure $KAu(CN)_2$ at 77 K upon excitation at 272 nm. According to Figure 3, batches 1 and 3 show the three aforementioned

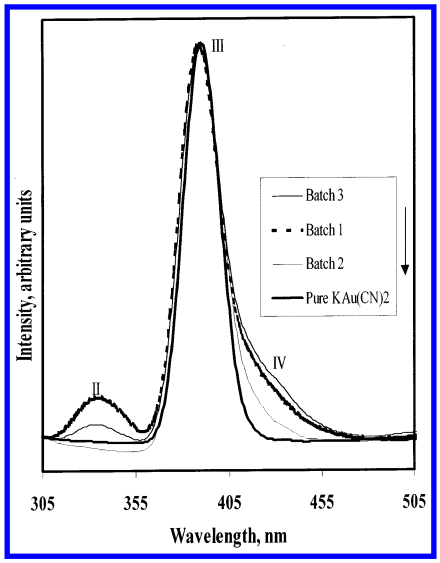

Figure 3. Emission spectra of pure $KAu(CN)_2$ and three batches of $KAu(CN)_2$/KCl crystals at 77 K, when excited at 272 nm. The spectra are shown for single crystals on going from batch 3 → batch 1 → batch 2 → pure $KAu(CN)_2$.

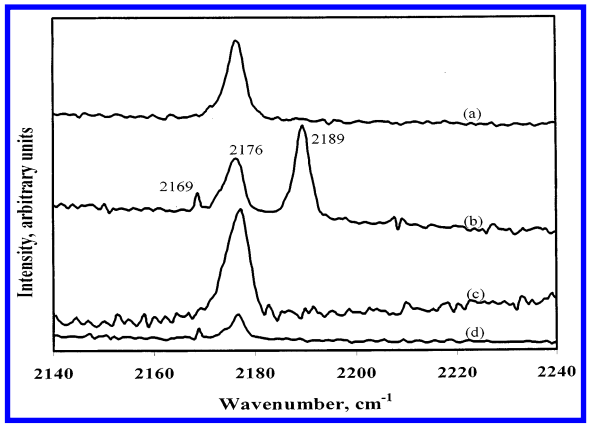

Figure 4. Raman spectra of single crystals of pure $KAu(CN)_2$ and three batches of $KAu(CN)_2$/KCl in the region of the cyanide stretching frequency. The spectra are shown for single crystals of pure $KAu(CN)_2$ (a), batch 3 (b), batch 2 (c), and batch 1 (d), respectively.

bands II and III, and IV. On the other hand, batch 2 and pure $KAu(CN)_2$ show only band III. Upon excitation at 315 nm, both batches 1 and 3 show bands III and IV whereas batch 2 and pure $KAu(CN)_2$ show only band III. These results indicate the presence of three emission sites in the mixed crystals with the lowest and highest Au content, whereas the crystals with intermediate Au content have only one emission site, similar to the situation in pure $KAu(CN)_2$ crystals. This trend was verified with a complete new set of crystals.

Lifetime measurements for the observed luminescence bands present in three batches of $KAu(CN)_2$/KCl and pure $KAu(CN)_2$ at 77 K are summarized in Table 1. The observed microsecond scale lifetimes for emission bands III and IV in each system suggests that these emissions are due to phosphorescent transitions, which are enhanced due to the large spin−orbit coupling of gold (spin−orbit coupling constant, ζ, for the 5d orbital of Au(I) is 5100 cm^{-1}).[40] It was not feasible to measure the lifetime for band II because of its very weak intensity with 266 nm laser excitation.

Raman Spectroscopy. Figure 4 shows the Raman spectra of the three batches of $KAu(CN)_2$/KCl as well as pure $KAu(CN)_2$ in the cyanide stretching frequency region. Batch 2 and pure $KAu(CN)_2$ have only one strong peak at ∼2176 cm^{-1} (traces c and a, respectively). Meanwhile, batch 1 (trace d) has two resolved peaks at ∼2169 and ∼2176 cm^{-1}, whereas batch 3 (trace b) has an additional peak at ∼2189 cm^{-1}. The appearance of the 2169 cm^{-1} peak for batches 1 and 3 (but not for batch 2 or pure $KAu(CN)_2$) is consistent with the appearance of the high-energy luminescence peak, II, only for these two batches (Figure 3).

There is a clear correlation between the Raman bands obtained for each sample and the corresponding photoluminescence spectra. Batch 2 and pure $KAu(CN)_2$ have virtually identical photoluminescence spectra and the Raman spectra of the two samples show a single *νCN* peak at the same frequency (2176 cm^{-1}). The presence of more than one peak other than 2176 cm^{-1} band in the *νCN* region indicates different sites for $[Au(CN)_2^-]$ ions in the KCl lattice. Therefore, the peaks at 2169, 2176, and 2189 cm^{-1} in Figure 4 are due to different $[Au(CN)_2^-]_n$ clusters present in the studied crystals. Gold−gold interactions are expected to strongly influence the C−N stretching vibration. On going from batch 1 →2→3, the relative intensity of the Raman peaks with higher *νCN* values increases, which is consistent with increased Au−Au interactions in the same direction. However, it is unusual that batch 3 has a Raman peak at a higher frequency (2189 cm^{-1}) than the 2176 cm^{-1} peak for pure $KAu(CN)_2$. An increase in gold−gold interactions leads to a decrease in back-bonding from gold to the antibonding π^* LUMO for the cyano group, hence a higher *νCN* value. This may result from either an increase in oligomerization (e.g., from dimers to trimers), or a shortening of the Au−Au distance in a given oligomer. The higher *νCN* value for batch 3 than for pure $KAu(CN)_2$ is likely due to a shorter Au−Au distance in the oligomer responsible for the dominant 2189 cm^{-1} band in batch 3 compared to the Au−Au distance between $[Au(CN)_2^-]$ species in the infinite layers of the pure compound. A somewhat similar situation has been encountered in a structural study by Schmidbaur et al. for various haloisonitrilegold(I) complexes.[41] It was found that compounds with infinite linear chain structures (i.e., polymers) showed longer Au−Au distances than those in more sterically encumbered compounds, which had oligomeric structures with shorter Au−Au distances.

To further validate the correspondence between the Raman and photoluminescence bands, single crystals of two batches of $[Ag(CN)_2^-]$/KCl as well as pure $KAg(CN)_2$ were also synthesized and spectroscopically analyzed. Upon excitation at 245 nm (Figure 5) and 275 nm (Figure 6), three different luminescence bands are observed for the $[Ag(CN)_2^-]$/KCl system. The relative intensities of these luminescence bands vary between the $[Ag(CN)_2^-]$/KCl batches and the results here reproduce the trends we reported previously for this doped system.[23−26] Pure $KAg(CN)_2$ shows only band C. The Raman spectra of these three samples are shown in Figure 7. Batch 1 shows 2 peaks at ∼2118 and ∼2124 cm^{-1}. Interestingly, the Raman spectrum of batch 2 (Figure 7b) shows an additional peak at ∼2159 cm^{-1} along with 2 peaks observed for batch 1. Pure $KAg(CN)_2$ shows only one Raman peak at ∼2159 cm^{-1}, which clearly correlates with band C in the luminescence spectra shown in Figures 5 and 6. Therefore, the observed additional Raman peak at ∼2159 cm^{-1} in batch 2 is assigned to the same species giving rise to luminescence band C. After a comparison of Figures 5, 6, and 7, the Raman bands observed at ∼2118 and ∼2124 cm^{-1} correlate with the observed luminescence bands A and B, respectively. Based on our discussion earlier that the stronger the metal−metal interactions the higher the frequencies in the Raman spectra and based on our luminescence bands assignment in Table 3 (vide infra), it is reasonable to

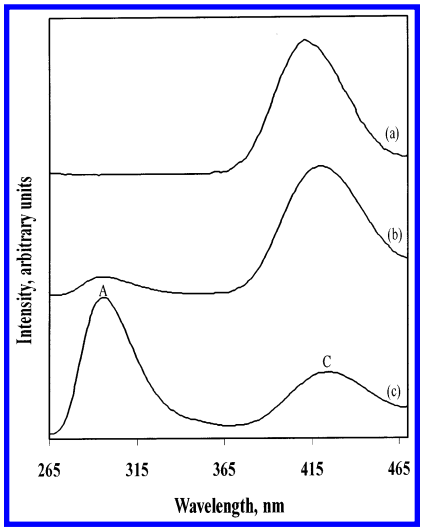

Figure 5. Emission spectra of pure $KAg(CN)_2$ and two batches of $KAg(CN)_2$/KCl crystals at 77 K, when excited at 245 nm. The spectra are shown for single crystals of pure $KAg(CN)_2$ (a), batch 2 (b), and batch 1 (c), respectively.

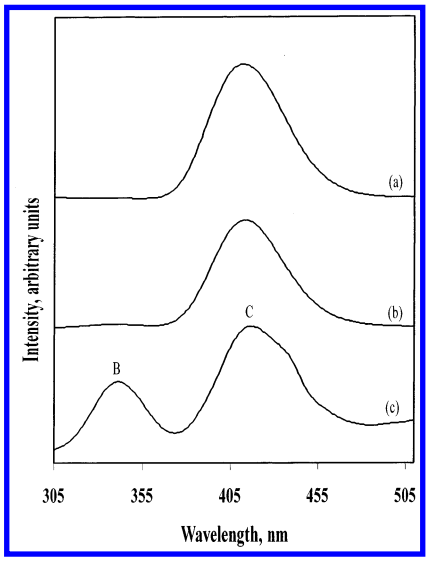

Figure 6. Emission spectra of pure $KAg(CN)_2$ and two batches of $KAg(CN)_2$/KCl crystals at 77 K, when excited at 275 nm. The spectra are shown for single crystals of pure $KAg(CN)_2$ (a), batch 2 (b), and batch 1 (c), respectively.

assign bands A and B to dimers and bent trimers, respectively. Because bent trimers have stronger metal−metal interactions than in dimers (as shown in Table 2, the bent trimer has a lower HOMO−LUMO gap than the dimer in both the ground and first excited states), and Raman peaks due to bent trimers should appear at higher frequencies. Therefore, the Raman peaks at ∼2124 and 2118 cm^{-1} are due to a bent trimer and a dimer, respectively. Luminescence band C is assigned to a linear trimer and correlates with the Raman band at ∼2159 cm^{-1}.

Table 1 shows the correlation between the luminescence and Raman bands for pure and doped crystals containing the dicyanoaurate(I) and dicyanoargentate(I) ions.

Extended Hückel (EH) Calculations. The preceding luminescence and Raman results clearly suggest the presence of multiple emission centers in solid-state systems of the dicyanoaurates(I). We believe that these centers are due to ground- and excited-state oligomers of $[Au(CN)_2^-]$. To characterize Au−Au interactions in relation to our experimental results, we have carried out EH calculations for different $[Au(CN)_2^-]_n$ oligomers

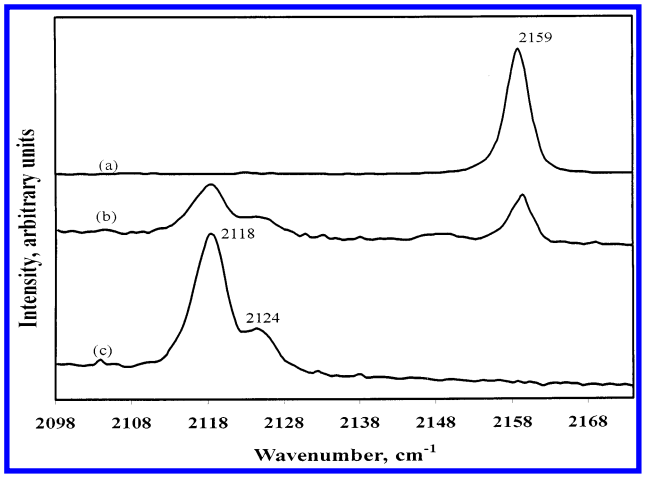

Figure 7. Raman spectra of single crystals of pure $KAg(CN)_2$ and two batches of $KAg(CN)_2$/KCl in the region of the cyanide stretching frequency. The spectra are shown for single crystals of pure $KAg(CN)_2$ (a), batch 2 (b), and batch 1 (c), respectively.

($n = 1-4$, eclipsed conformations). The results are summarized in Table 2 for free and doped oligomers. We shall discuss first the ground state and first excited-state calculations for free oligomers of $[Au(CN)_2^-]$ units. The data indicate that the aurophilic bonding and the electronic transition energies are both sensitive to the number of ions (n) in the oligomers as well as the geometry and conformation of the ions in the oligomer. For example, ground-state calculations for linear eclipsed oligomers reveal that as "n" increases from 2 → 3 → 4, the binding energy increases from 0.13 → 0.30 → 0.44 eV, and the HOMO−LUMO gap decreases from 3.78 → 3.43 → 3.34 eV. Table 2 also shows that bent and linear trimers gave significantly different results, suggesting that different geometries in a given oligomer lead to differences in Au−Au bonding and electronic energies.

Table 2 also shows that for any given $[Au(CN)_2^-]_n$ oligomer, the excited state has a deeper potential well (higher binding energy), higher Au−Au overlap population, shorter Au−Au equilibrium distance than the corresponding ground state. For example, a ground-state dimer has a binding energy of 0.13 eV, whereas the corresponding value for the excited state is 0.88 eV. It is therefore concluded that, for all $[Au(CN)_2^-]_n$ oligomers, Au−Au bonding is stronger in the first excited state than in the corresponding ground state. Stronger Au−Au bonding in the first excited state than in the ground state is an indication of the formation of $^*[Au(CN)_2^-]_n$ excimers and exciplexes. The example shown in Figures 8 illustrates the strong Au−Au bonding and low electronic energy for exciplexes compared to ground-state oligomers. The low energies, large Stokes shifts, and structureless features of the emission bands (even at cryogenic temperatures in doped single crystals) are consistent with the exciplex assignment for the emission bands of the systems described here, which the aforementioned calculations reinforce. Supporting evidence of this assignment, including characterization of the bonding in the triplet excimer in staggered $^*[Au(CN)_2^-]_2$ by modern UHF/MP2 calculations, has been published elsewhere.[10]

Ground-state EH calculations have also been performed for the monomers, and eclipsed dimers doped in a modeled KCl lattice. Results of these calculations are summarized in Table 2. Comparison of the free $[Au(CN)_2^-]$ monomer versus the doped monomer in Table 2 shows that both the HOMO and LUMO undergo destabilization by doping the monomer in the KCl lattice. This is likely due to the crystal field of the Cl^-

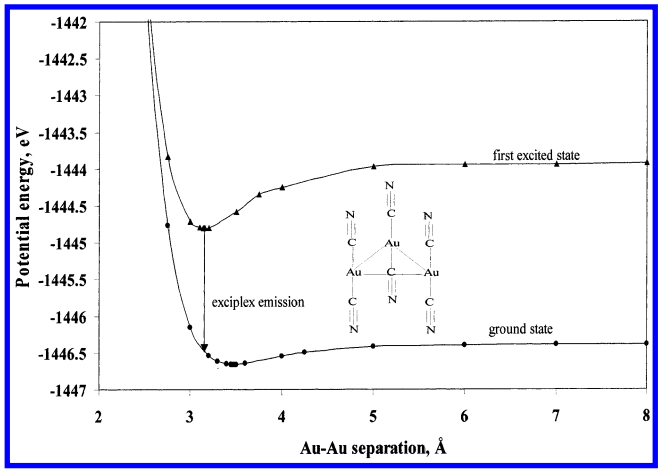

Figure 8. Ground and first excited-state potential energy diagrams for bent $[Au(CN)_2^-]_3$.

ions in the KCl lattice. According to Table 2, doping the $[Au(CN)_2^-]$ monomer in the KCl lattice results in a reduction of the energy difference between the HOMO and the LUMO. This gives a possible explanation for observing lower energy excitation bands in the doped system compared to the lowest energy absorption band observed in dilute aqueous $KAu(CN)_2$ solutions.[36,39] Table 2 also shows that as one proceeds from $[Au(CN)_2^-] \rightarrow [Au(CN)_2^-]_2$, the HOMO−LUMO gap decreases from 4.09 → 4.04 eV due to the presence of ground-state interactions. Accurate information about the extent of Au−Au bonding and optical energies among various doped oligomers were not possible because of the very large lattice energy of the KCl crystal, which masks the much weaker Au−Au interactions in the EH calculations.[42]

Exciplex Tuning. A given doped crystal of $[Au(CN)_2^-]$/KCl exhibits multiple emission bands. For example, a single crystal from batch 1 displays three emission bands that span an emission range of more than 11 000 cm^{-1} (Figure 1). Because these bands are due to metal−metal bonded exciplexes, the results here represent further examples of the "exciplex tuning" phenomenon, which was described earlier for doped crystals of $[Ag(CN)_2^-]$/KCl [23−26] and solutions of both $K[Au(CN)_2]$ and $K[Ag(CN)_2]$.[10] Exciplex tuning in a doped crystal of $[Au(CN)_2^-]$/KCl can be achieved by site-selective excitation (Figure 1) and by varying the dopant concentration (Figure 3) in a manner similar to that described for doped crystals of $[Ag(CN)_2^-]$/KCl.[23−26] Site-selective excitation is used to resolve the different emission bands from one another (Figures 1 and 2), whereas varying the dopant concentration is used to maximize the relative intensity of a given exciplex band (Figures 3). For example, $[Au(CN)_2^-]$/KCl crystals with the highest Au content (batch 3) show three emission bands at 335, 390, and 425 nm upon excitation at 272 and 315 nm, whereas crystals with a lower Au content (batch 2) show only one band at 390 nm regardless of the excitation wavelength.

Exciplex tuning of the dicyanoaurate(I) emission is seen in various doped crystals, pure crystals, and solutions. The tuning action is achieved by varying the excitation wavelength and temperature in any of these media, the dopant concentration and host alkali halide crystal in doped crystals, the counterion in pure crystals, and concentration and solvent in solutions.[43] Although effective tuning can be achieved in any of these systems alone, the tuning range can be expanded over a wider emission energy range if one combines the results of the various media. To illustrate, we show in Figure 9 selected emission spectra of various dicyanoaurate(I) species at different conditions. Several exciplex emission bands are obtained from regions in the far UV (∼270 nm) to the orange (∼660 nm), i.e., spanning an energy range of ∼22 000 cm^{-1} with this approach.[44] Similar tuning was achieved for the dicyanoargentate(I) emission.[23−26,45]

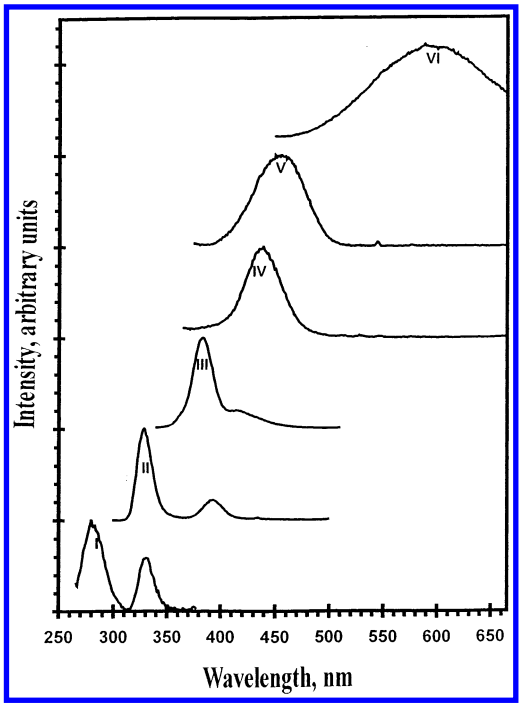

Figure 9. Exciplex tuning of the dicyanoaurate(I) emission in different media. Bands shown are I, 1.00×10^{-5} M $KAu(CN)_2$ frozen solution in methanol (77 K, $\lambda_{ex} = 250$ nm); II, 1.00×10^{-4} M $KAu(CN)_2$ frozen solution in methanol (77 K, $\lambda_{ex} = 260$ nm); III, $KAu(CN)_2$/KCl doped crystal (11 K, $\lambda_{ex} = 265$ nm); IV, $KAu(CN)_2$/KCl doped crystal (120 K, $\lambda_{ex} = 350$ nm); V, 0.200 M $KAu(CN)_2$ aqueous solution (ambient temperature, $\lambda_{ex} = 320$ nm); and VI, $KAu(CN)_2$ pure crystal (ambient temperature, $\lambda_{ex} = 330$ nm).

The various emission bands seen in Figure 9 are assigned to $^*[Au(CN)_2^-]_n$ exciplexes with different "*n*", configuration, and/or geometry. The exact identity of each exciplex cannot be determined with a great certainty. A reasonable assignment is suggested in Table 3 based on correlating the trends of luminescence energies seen in various dicyanoaurate(I) species (solutions with various concentrations, doped crystals with different dopant concentrations, and pure crystals), the Raman data and the trends of electronic energies for various $[Au(CN)_2^-]_n$ oligomers obtained from the electronic structure calculations described above.

We are aware of three literature precedents in which the emission energies of the same or similar complexes have been tuned significantly. Efficient tuning of the emission of the tetracyanoplatinates (II) is achieved by a combination of chemical substitution (changing the counterion) and application of high pressure in order to significantly change the Pt−Pt distances.[27,28] Another example involves Pt(diimine)(dithiolate) complexes, whose charge-transfer emission energies have been tuned by 7400 cm^{-1} by varying the ligands and their substituents.[29] More recently, Balch and co-workers have described an example in which the emission energy for frozen solutions of the complex $[Au\{C(NHMe)_2\}_2]^+$ has been tuned to different visible colors by variation of the solvent and counterion.[46] The tuning we achieve for the dicyanoaurate(I) and dicyanoargentate(I) ions, as described above, competes favorably with all these examples and spans a wider emission energy range.

Conclusions

This study illustrates interesting luminescence behavior of dicyanoaurates(I) doped in a KCl host lattice. Three luminescence bands are observed in the $[Au(CN)_2^-]$/KCl system, whereas only one band is observed in the pure $KAu(CN)_2$ system excited with the same wavelengths. The luminescence in the $[Au(CN)_2^-]$/KCl system can be tuned by varying the excitation wavelength or by varying the dopant concentration. By increasing the dopant concentration of $[Au(CN)_2^-]$, our spectroscopic data predict that the oligomer size increases. At the highest dopant concentration, the Au−Au bond distance is shorter than the corresponding value for the pure $KAu(CN)_2$. On the other hand, in the $[Ag(CN)_2^-]$/KCl system, the oligomer size increases with increasing dopant concentration of $[Ag(CN)_2^-]$ and at the highest dopant levels, the Ag−Ag bond distance is similar to the value of pure $KAg(CN)_2$. We demonstrate efficient tunability of ∼22,000 cm^{-1} in various $Au(CN)_2^-$ systems.

Because observed luminescence bands are due to different orientations and different aggregations of $[Au(CN)_2^-]$ units, Raman spectroscopy can be correlated with the measured photoluminescence spectra. Three emission bands observed for a single crystal of batch 3 of the $[Au(CN)_2^-]$/KCl system shows three peaks in the ν_{CN} region of the Raman spectrum giving a reasonable correlation among Raman and luminescence spectroscopic results. Extended Hückel calculation predictions give good agreement with the observed experimental results.

Acknowledgment. We thank the donors of the Petroleum Research Fund, administered by the American Chemical Society, for support of this research. M.A.O. acknowledges the Robert A. Welch foundation of Houston, Texas, for supporting his contribution.

References and Notes

(1) (a) Pyykkö, P. *Chem. Rev*. **1997**, *97*, 597. (b) Pyykkö, P.; Zhao, Y. *Angew. Chem., Int. Ed. Engl.* **1995**, *34*, 1894. (c) Pyykkö, P.; Li, J.; Runeberg, N. *Chem. Phys. Lett.* **1994**, *218*, 133. (d), Pyykkö P.; Zhao, Y.; *Chem. Phys. Lett.* **1991**, *177*, 103. (e) Rösch, N.; Görling, A.; Ellis, D. E.; Schmidbaur, H. *Angew. Chem., Int. Ed. Engl.* **1989**, *28*, 1357. (f) Burdett, J. K.; Eisenstein, O.; Schweizer, W. B. *Inorg. Chem*. **1994**, *33*, 3261.

(2) (a) Schmidbaur, H. *Chem. Soc. Rev*. **1995**, 391. (b) Schmidbaur, H. *Interdiscip. Sci. Rev.* **1992**, *17*, 213. (c) Schmidbaur, H. *Gold Bull.* **1990**, *23*, 211.

(3) (a) Vickery, J. C.; Balch, A. L. *Inorg. Chem.* **1997**, *36*, 5978. (b) Calcar, P. M. V.; Olmstead, M. M.; Balch, A. L. *J. Chem. Soc., Chem. Commun*. **1995**, 1773.

(4) (a) Puddephatt, R. *J. Chem. Commun.* **1998**, 1055. (b) The Chemistry of Gold; Elsevier: Amsterdam, 1978.

(5) (a) Fernández, E. J.; López-de-Luzuriaga, J. M.; Monge, M.; Rodríguez, M. A.; Crespo, O.; Gimeno, M. C.; Laguna, A.; Jones, P. G. *Inorg. Chem.* **1998**, *37*, 6002. (b) Gimeno, M. C.; Laguna, A. *Chem. Rev*. **1997**, *97*, 511.

(6) (a) Mingos, D. M. P.; Yau, J.; Menzer, S.; Williams, D. *J. Angew. Chem., Int. Ed. Engl.* **1995**, *34*, 1894. (b) Mingos, D. M. P. *J. Chem. Soc., Dalton Trans*. **1996**, 561.

(7) (a) Shieh, S.-J.; Hong, X.; Peng, S.-M.; Che, C.-M. *J. Chem. Soc., Dalton Trans.* **1994**, 3067. (b) Tzeng, B.-C.; Cheung, K.-K.; Che, C.-M. *Chem. Commun*. **1996**, 1681. (c) Tzeng, B.-C.; Che, C.-M.; Peng, S.-M. *Chem. Commun*. **1997**, 1771.

(8) (a) Davila, R. M.; Elduque, A.; Grant, T.; Staples, R. J.; Fackler, J. P., Jr. *Inorg. Chem.* **1993**, *32*, 1749. (b) Davila, R. M.; Staples, R. J.; Elduque, A.; Harlass, M.; Kyle, L.; Fackler, J. P. Jr.. *Inorg. Chem.* **1994**, *33*, 5940.

(9) (a) Leung, K. H.; Phillips, D, L.; Tse, M, C.; Che, C. M.; Miskowski. *J. Am. Chem. Soc*. **1999**, *121*, 4799. (b) Che, C. M.; Tse, M. C.; Chan, M. C. W.; Cheung, K. K.; Philips, D. L.; Leung, K. H. *J. Am. Chem. Soc*. **2000**, *122*, 2464.

(10) Rawashdeh-Omary, M. A.; Omary, M. A.; Patterson, H. H.; Fackler, J. P., Jr. *J. Am. Chem. Soc*. **2001**, *123*, 11 237.

(11) Shaw, C. F., III. The Biochemistry of Gold. In *Gold: Progress in Chemistry, Biochemistry and Technology*; Schmidbaur, H., Ed.; Wiley: Chichester, New York, 1999, Chapter 10.

(12) (a) Higby, G. J. *Gold Bulletin*, **1982**, *15*, 130. (b) Kean, W. F.; Lock, C. J. L.; Howard-Lock, H. *Inflammopharmacology* **1991**, *1*, 103.

(13) (a) Grässle, G. E.; Hiller, W.; Strähle, J. *Z. anorg. Allg. Chem*. **1983**, *504*, 29. (b) Biltz, W.; Wein, W. . *Z. anorg. Allg. Chem*. **1925**, *148*, 192.

(14) Mansour, M. A.; Connik, W. B.; Lachicotte, R. J.; Gysling, H. J.; Eisenberg, R. *J. Am. Chem. Soc*. **1998**, *120*, 1329.

(15) Blonder, R.; Levi, S.; Tao, G.; Ben-Dov, I.; Willner, I. *J. Am. Chem. Soc*. **1997**, *119*, 10 467.

(16) Wolf, M. O.; Fox, M. A. *J. Am. Chem. Soc*. **1995**, *117*, 1845.

(17) (a) Lowry, T. H.; Schuller-Richardson, K. *Mechanism and Theory in Organic Chemistry*; Harper & Row: New York, 1981; pp 919−925. (b) Turro, N. J. *Modern Molecular Photochemistry*; Benjamin/ Cummings: Menlo Park, CA, 1978; pp 135−146.(c) Lamola, A. A. In *energy transfer and Organic Photochemistry*; Lamola, A. A., Turro, N. J., Eds.; Wiley-Interscience: New York, 1969; pp 54−60. (d) *The exciplex;* Gordon, M., Ware, W. R., Eds; Academic Press: New York, 1975. (e) Kopecky, J. *Organic Photochemistry: A Visual Approach*; VCH: New York, 1991; pp 38−40. (f) Michl, J.; Bonacic-Koutecky, V. *Electronic Aspects of Organic Photochemistry*; Wiley: New York, 1990; pp 274−286.

(18) For a recent review see: Horváth, A.; Stevenson, K. L. *Coord. Chem. Rev*. **1996**, *153*, 57.

(19) Shin, K. K.; Barrie, J. D.; Dunn, B.; Zink, J. I. *J. Am. Chem. Soc*. **1990**, *112*, 5701.

(20) Barrie, J. D.; Dunn, B.; Hollingsworth, G.; Zink, J. I. *J. Phys. Chem.* **1989**, *93*, 3958.

(21) (a) Clodfelter, S. A.; Doede, T. M.; Brennan, B. A.; Nagle, J. K.; Bender, D. P.; Turner, W. A.; Lapunzia, P. M. *J. Am. Chem. Soc*. **1994**, *116*, 11 379. (b) Nagle, J. K.; Brennan, B. A. *J. Am. Chem. Soc.* **1988**, *110*, 5931.

(22) Pettijohn, C. N.; Chuong, B.; Nagle, J. K.; Voglar, A. *Coord. Chem. Rev.,* **1998**, *171*, 85.

(23) Omary, M. A.; Patterson, H. H. *J. Am. Chem. Soc*. **1998**, *120*, 7696.

(24) Omary, M. A.; Hall, D. R.; Shankle, G. E.; Siemiarczuk, E.; Patterson, H. H.*J. Phys. Chem. B* **1999**, *103*, 3845.

(25) Rawashdeh-Omary, M. A.; Omary, M. A.; Shankle, G. E.; Patterson, H. H. *J. Phys. Chem. B.* **2000**, *104*, 6143.

(26) Patterson, H. H.; Kanan, S. M.; Omary, M. A. *Coord. Chem. Rev*. **2000**, *208*, 227.

(27) Yersin, H.; Gliemann, G. *Ann. N. Y. Acad. Sci*. **1978**, *313*, 539.

(28) Gliemann, G.; Yersin, H. *Struct. Bonding* **1985**, *62*, 87, and references therein.

(29) Cummings, S. D.; Eisenberg, R. *J. Am. Chem. Soc*. **1996**, *118*, 1949.

(30) Meyer, T. J. *Acc. Chem. Res*. **1989**, *22*, 163.

(31) Rawashdeh-Omary, M. A.; Larochelle, C. L.; Patterson, H. H. *Inorg. Chem*. **2000**, *39*, 4527.

(32) Kanan, S. M.; Omary, M. A.; Patterson, H. H.; Matsuoka, M. Anpo, M. *J. Phys. Chem. B.* **2000**, *104*, 3507.

(33) Kanan, S. M.; Kanan, M. C.; Patterson, H. H. *J. Phys. Chem. B.* **2001**, *105*, 7508.

(34) Kanan, S. M.; Tripp, C. P.; Austin, R. A.; Patterson, H. H. *J. Phys. Chem. B.* **2001**, *105*, 9441.

(35) Nagasundaram, N.; Roper, G.; Biscoe, J.; Chai, J. W.; Patterson, H. H.; Blom, N.; Ludi, A. *Inorg. Chem.* **1986**, *25*, 2947−2950.

(36) Rawashdeh-Omary, M. A.; Omary, M. A.; Patterson, H. H. *J. Am. Chem. Soc.* **2000**, *122*, 10 371.

(37) Omary, M. A.; Patterson, H. H.; Shankle, G. E. *Mol. Cryst. Liq. Cryst.* **1996**, *284*, 399.

(38) Shanon, R. D. *Acta Crystallogr*. **1976**, *A32*, 751.

(39) Mason, W. R. *J. Am. Chem. Soc*. **1973**, *95*, 3573.

(40) Griffith, J. S. *Theory of Transition Metal Ions,* Cambridge University Press: Cambridge, 1964.

(41) Schneider, W.; Angermaier, K.; Sladek, A.; Schmidbaur, H. Z. *Naturforsch. B.* **1996**, *51*, 790.

(42) The calculated binding energy for $[Au(CN)_2^-]_2$ in KCl is 5.1 eV (Table 2). This value is too large to be attributed to Au−Au interactions because such interactions are typically 0.2−0.5 eV. Therefore, the extremely high binding energy of $[Au(CN)_2^-]_2$ dimer in KCl cannot be explained based on Au−Au interactions. The calculated Au−Au equilibrium distance for $[Au(CN)_2^-]_2$ dimer in KCl is 4.5 Å, which corresponds to the intercationic distance in the KCl lattice. The large stabilization of the $[Au(CN)_2^-]_2$ dimer in the KCl lattice is, therefore, mostly due to the lattice energy of the ionic crystal. The lattice energy of KCl is 7.1 eV (Huheey, J.; Keiter, E.; Keiter, R. *Inorganic Chemistry*; Harper Collins College: New York, 1993).

(43) Rawashdeh-Omary, M. A., Ph.D. Thesis, Graduate School, The University of Maine, Orono, Maine, 1999.

(44) The limits are based on emission energies at half-maxima for bands I and VI in Figure 9.

(45) Omary, M. A., Ph.D. Thesis, Graduate School, The University of Maine, Orono, Maine, 1997.

(46) White-Morris, R. L.; Olmstead, M. M.; Jiang, F.; Tiniti, D. S.; Balch, A. L. *J. Am. Chem. Soc.* **2002**, *124*, 2327.